ANTIMICROBIAL AGENTS AND CHEMOTHERAPY, May 2009, p. 2100–2109 Vol. 53, No. 5
0066-4804/09/$08.00+0 doi:10.1128/AAC.01197-08

Molecular Genetics of *para*-Aminosalicylic Acid Resistance in Clinical Isolates and Spontaneous Mutants of *Mycobacterium tuberculosis*▽†

Vanessa Mathys,[1,5] René Wintjens,[4,5] Philippe Lefevre,[1] Julie Bertout,[2] Amit Singhal,[1] Mehdi Kiass,[1] Natalia Kurepina,[3] Xiao-Ming Wang,[1] Barun Mathema,[3] Alain Baulard,[2] Barry N. Kreiswirth,[3] and Pablo Bifani[1]*

Laboratory of Molecular Pathology of Tuberculosis, Pasteur Institute, Scientific Institute of Public Health, Brussels, Belgium[1]; Inserm U629, Pasteur Institute, Lille, France[2]; Tuberculosis Center, Public Health Research Institute, University of Medicine and Dentistry, Newark, New Jersey, 07103[3]; Laboratoire de Chimie Générale, Institute of Pharmacy, Université Libre de Bruxelles, Brussels, Belgium[4]; and Fond National de la Recherche Scientifique (FNRS), Brussels, Belgium[5]

Received 9 September 2008/Returned for modification 16 October 2008/Accepted 12 February 2009

The emergence of *Mycobacterium tuberculosis* resistant to first-line antibiotics has renewed interest in second-line antitubercular agents. Here, we aimed to extend our understanding of the mechanisms underlying para-aminosalicylic acid (PAS) resistance by analysis of six genes of the folate metabolic pathway and biosynthesis of thymine nucleotides (*thyA*, *dfrA*, *folC*, *folP1*, *folP2*, and *thyX*) and three *N*-acetyltransferase genes [*nhoA*, *aac(1)*, and *aac(2)*] among PAS-resistant clinical isolates and spontaneous mutants. Mutations in *thyA* were identified in only 37% of the clinical isolates and spontaneous mutants. Overall, 24 distinct mutations were identified in the *thyA* gene and 3 in the *dfrA* coding region. Based on structural bioinformatics techniques, the altered ThyA proteins were predicted to generate an unfolded or dysfunctional polypeptide. The MIC was determined by Bactec/Alert and dilution assay. Sixty-three percent of the PAS-resistant isolates had no mutations in the nine genes considered in this study, revealing that PAS resistance in *M. tuberculosis* involves mechanisms or targets other than those pertaining to the biosynthesis of thymine nucleotides. The alternative mechanism(s) or pathway(s) associated with PAS resistance appears to be PAS concentration dependent, in marked contrast to *thyA*-mutated PAS-resistant isolates.

The discovery of the antitubercular activity of para-aminosalicylic acid (PAS) by Lehmann in 1943 (15) was followed by two successful clinical trials conducted in 1944 and 1949 (16, 31). These breakthroughs, combined with the almost simultaneous discovery and introduction of streptomycin (STR), brought much hope in the fight against tuberculosis (TB) (22). The initial success was soon thwarted by the emergence of PAS and STR resistance. This was overcome by coadministering PAS and STR, resulting in the advent of combination therapy (19). In 1951, isoniazid was added to anti-TB regimens until the mid-1960s. Although including PAS combination therapy proved efficacious, side effects attributed to PAS were documented as early as 1951 (6, 25). In addition to PAS-associated gastrointestinal toxicity, elevated and repetitive dosing complicated therapeutic regimens. PAS therapy was discontinued after the introduction of rifampin (rifampicin) and pyrazinamide. PAS was reintroduced in the United States in 1992, following several outbreaks of multidrug-resistant (MDR) isolates (4). Since then, the need for new antibiotics for the treatment of MDR TB has led to the development of novel formulations of PAS, which have proven to be less toxic (5). Today, PAS is used primarily as a second-line drug to treat MDR TB (34).

PAS has structural similarities to sulfonamides. Sulfonamides are structural analogues of para-aminobenzoic acid, the substrate of dihydropteroate synthase (encoded by *folP1*/*folP2*), and hence function as competitive inhibitors. FolP1 and its putative homologue FolP2 catalyze the condensation of para-aminobenzoic acid and 6-hydroxymethyl-7,8-dihydropterein pyrophosphate to 7,8-dihydropteroate, which is converted to dihydrofolate and reduced to generate the cofactor tetrahydrofolate (THF) by the enzyme dihydrofolate reductase (encoded by *dfrA*) (Fig. 1). Unlike the actions of some sulfonamides or analogues in other pathogens, the PAS-inhibitory activity of *folP1* has proven to be unexpectedly poor in vitro (24). More recently, Rengarajan and colleagues (26), using transposon mutagenesis, have shown that PAS resistance is associated with mutations of thymidylate synthase A, encoded by the *thyA* gene and required for thymine biosynthesis in the folate pathway. This result implies that PAS functions as a folate antagonist, a suggestion supported by the identification of mutations within the *thyA* coding region in PAS-resistant (PAS^r) clinical isolates (26).

ThyA catalyzes the reductive methylation of dUMP to yield dTMP, required for de novo dTTP synthesis (12). ThyA requires the 5,10-methylene THF cofactor both as a reductant and as a carbon donor in the methylation reaction. The presence of the *thyX* gene, encoding a functional homologue of thymidylate synthase but with the clear distinction that it utilizes flavin adenine dinucleotide as a cofactor instead of THF,

* Corresponding author. Present address: Novartis Institute for Tropical Diseases (NITD), TB Unit, 10 Biopolis Road, 05-01 Chromos, Singapore 138670, Singapore. Phone: 6567223526. Fax: 6567222917. E-mail: Pablo.bifani@novartis.com.

† Supplemental material for this article may be found at http://aac.asm.org/.

▽ Published ahead of print on 23 February 2009.

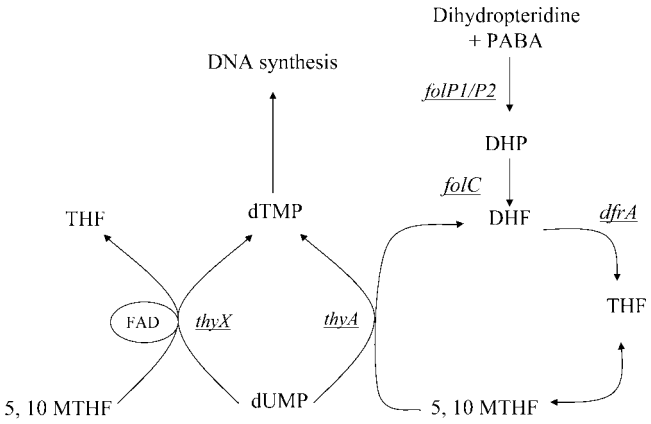

FIG. 1. The folate pathway and plausible targets for PAS inhibition. The six genes analyzed in this study are underlined.

in the *Mycobacterium tuberculosis* genome is noteworthy (8). Although ThyX utilizes flavin adenine dinucleotide as a cofactor, it still requires 5,10-methylene THF as the methyl donor. It is hypothesized that the bacteriostatic activity of PAS results from perturbation of the folate pathway, although the underlying mechanism has yet to be elucidated (26).

Here, we set out to investigate the mutations associated with PAS resistance in a collection of well-characterized *M. tuberculosis* clinical isolates and PAS^r spontaneous mutants. Five genes, *thyA*, *dfrA*, *folC*, *folP1*, and *folP2*, encoding enzymes of the folate pathway; *thyX*, encoding an alternative thymine-biosynthetic enzyme; and three *N*-acetyltransferase genes possibly associated with the modification of PAS were analyzed. To better understand PAS resistance, the identified mutations were correlated with MICs and the protein three-dimensional (3D) structure. The structural stability was modeled for all mutants. To our surprise, only 37% of the PAS^r clinical isolates or spontaneous mutants encoded mutations in enzymes of the folate pathway, indicating that other mechanisms associated with PAS resistance have yet to be elucidated.

MATERIALS AND METHODS

***M. tuberculosis* laboratory reference strains.** The laboratory PAS^r mutant and PAS-susceptible (PAS^s) H37Rv strains were used as positive and negative controls, respectively (Table 1) (3, 29, 30). *M. tuberculosis* complex strains used as reference strains included *Mycobacterium bovis* (TMC 401-Ravenel-PAS^r, TMC 410-NADL-PAS^r, and TMC 407-Branch-PAS^s), *M. bovis*-BCG-Pasteur (ATCC 35734-PAS^s), *Mycobacterium africanum* PAS^s (TMC 5122), and *Mycobacterium microti* PAS^s (ATCC 19422).

***M. tuberculosis* clinical isolates.** Twenty-six PAS^r clinically unrelated isolates were selected from the *M. tuberculosis* collection ($n > 25{,}000$) maintained at the Tuberculosis Center, Public Health Research Institute, Newark, NJ (PHRI), for PAS^r phenotypic and genotypic analyses (Table 1). These PAS^r clinical isolates were selected for their genetic diversity and as representatives of the nine major *M. tuberculosis* phylogenetic clusters as determined by Gutacker et al. (10). In addition to the 26 diverse clinical isolates, representative samples from three strain clusters (related isolates belonging to the *M. tuberculosis* genotypes P, AB, and AU) associated with three unrelated MDR outbreaks in New York City (2, 21) were also analyzed. Representative P strains comprised 15 MDR-PAS^r and 1 MDR-PAS^s isolates. Three PAS^r and one PAS^s AB isolates and five AU clustered strains were analyzed. The AU isolates were MDR and polyresistant, but only one isolate had a PAS^r phenotype (2).

All of the isolates were typed by multiple genetic techniques in order to establish their genetic diversity (unrelated clinical isolates) or relatedness (clustered clinical isolates). The nomenclature used for the classification of the strains was based first on IS*6110* restriction fragment length polymorphism patterns, followed by other genotyping techniques as described elsewhere (Table 1) (18).

Selection of spontaneous PAS^r mutants. Spontaneous mutants resistant to PAS were selected on 7H11 plates containing 16 μg/ml of PAS (Sigma). To avoid strain bias, spontaneous mutants of eight well-characterized clinical strains (W4, J, CDC1551, OO6, BE, AF AU, and AI) were used. The protocol for selection of spontaneous mutants was adapted from Luria and Delbruck (17) and Morlock et al. (20). Briefly, for each of the eight strains, a sample was cultured under standard conditions in Sauton medium for 3 weeks, the bacterial density was adjusted to an optical density at 600 nm of 1.2 (approximately 7.2×10^7 CFU/ml), and bacteria were inoculated into 220 individual tubes (5 ml Sauton broth each; no antibiotic) for 32 days and plated in toto on 7H11 plates containing 16 μg/ml PAS. Colonies were picked and subcultured in the presence of various concentrations of PAS for determination of the MIC, followed by DNA extraction and stocking. Only a single colony per plate was picked for this study.

Sequencing drug target regions. The loci including the *folP1* (Rv3608c), *folP2* (Rv1207), *thyX* (Rv2754c), *dfrA* (Rv2763c), and *thyA* (Rv2764c) genes and the corresponding 100 nucleotides (nt) upstream were sequenced in both directions for all isolates. The putative bifunctional *M. tuberculosis* dihydrofolate synthetase-folylpolyglutamate synthetase gene, known as *folC* (Rv2447c), was sequenced in 12 PAS^r isolates that did not include any other mutations in genes of the folate biosynthetic pathway. Three additional genes were further sequenced in five of these PAS^r isolates, including the arylamine *N*-acetyltransferase gene, *nhoA* (Rv3566c); the aminoglycoside 2′-*N*-acetyltransferase gene, *aac(1)* (Rv0262); and the aminoglycoside *N*-acetyltransferase (GCN5-related *N*-acetyltransferase) gene, *aac(2)* (Rv1347c). A complete list of the sequencing primers can be found in Table S1 in the supplemental material. Amplicon sequencing was outsourced.

MIC. The MICs of all the clinical strains and spontaneous mutants were determined by the agar dilution method and BacT/Alert 3D system (bioMérieux, France). Briefly, samples (10^7 CFU/ml; diluted 1:100; 100 μl plated) were plated simultaneously on 7H11 plates containing 0, 16, 32, 64, and 128 μg/ml of PAS, and the colony formation was tabulated. Likewise, MICs were determined using the BacT/Alert 3D system as recommended by the supplier. Finally, bacillary growth was monitored spectrophotometrically (optical density at 600 nm) every 72 h for 32 consecutive days in triplicate. Growth curves were determined for four to six strains per group, including clinical isolates ($n = 6$), spontaneous mutants with an early stop codon in the *thyA* gene ($n = 2$) or with other mutations within the *thyA* gene ($n = 6$), and PAS^r isolates including wild-type genes in the folate and pyrimidine biosynthesis pathway ($n = 6$). Growth curves were done on 7H9 broth in the presence of 0, 16, 32, 64, and 128 μg/ml of PAS.

Structural analysis and homology modeling. A 3D model of the *M. tuberculosis* thymidylate synthase homodimer was built with the automated comparative-modeling program Modeler v8.2 (27) using the very high-resolution X-ray structure of *Escherichia coli* thymidylate synthase as a homologous protein template (Protein Data Bank entry 2G8O; X-ray resolution, 1.3 Å). The stereochemical quality of the model was evaluated with the procheck-nmr program (14). The Naccess program (11) was used to identify buried and solvent accessible residues. Residues interacting with the substrate or cofactor were defined using the Ligplot program (33) based on the X-ray structure of *E. coli* thymidylate synthase, which was cocrystallized with the substrate dUMP and the cofactor 10-propargyl-5,8-dideazafolate, an analogue of THF (23). Thermodynamic stability changes resulting from a single-site mutation were predicted using the PoPMuSiC web server (13). This program computes the free-energy difference (ΔG) for a given protein between its folded and unfolded states and evaluates the changes ($\Delta\Delta G$) in this unfolding free-energy difference upon mutations. A positive $\Delta\Delta G$ indicates that the mutation is predicted to thermodynamically decrease the protein stability. Conversely, a negative $\Delta\Delta G$ predicts a mutant protein more stable than the wild type. The magnitude of the predicted $\Delta\Delta G$ is also important for estimating the reliability of predictions, as the errors of the PoPMuSiC program are evaluated to be on the order of ± 0.3 to 0.4 kcal/mol for mutations of solvent-accessible residues and to be on the order of ± 1.2 to 1.9 kcal/mol for mutations of buried residues (7). Finally, at each mutated position, the conservation of wild-type residues and the occurrence of mutant residues were evaluated on an alignment of 279 thymidylate synthase sequences. These sequences were retrieved by a BLAST query (1) and were aligned using the ClustalX program (32).

RESULTS

Polymorphism in the enzymes of the folate metabolic pathway and thymine biosynthesis in clinical isolates and spontaneous mutants. The *thyA*, *thyX*, *dfrA*, *folP1*, and *folP2* genes

TABLE 1. Molecular characteristics and drug susceptibility profiles of isolates studied

FP[a]	TN[b]	ORI[c]	No. of IS*6110*[d]	PGG[e]	Cluster[f]	Spoligo (octal)[g]	Resistance[h]	
							First line	Second line
Unclustered clinical isolates								
A7	6196	US	7	2	III	777777777720771	INH, RIF, EMB, PZA, STR	ETH, KAN, PAS
CC3	4469	US	12	2	VI	′776177607760771	INH, RIF, EMB, PZA, STR	ETH, PAS
CI12	18117	KS	15	1	II	′000000000003771	INH, EMB	PAS
CI1	4862	US	10	1	II	000000000000771	INH, RIF, EMB, STR	CIP, PAS
H	14905	CH	2	2	IV	777776777760601	INH, RIF, PZA	RBT, RMC, PAS
H	13528	IN	2	2	IV	777776777760601	INH, RIF, EMB, PZA	PAS
H	16213	US	2	2	IV	777776777760601	INH	PAS
BA27	14204	HA	13	2	VI	′777777607760771	INH	PAS
BA19	14303	US	12	2	VI	677777607760771	INH	PAS
BA19	14550	US	12	2	VI	677777607760771	INH	PAS
BA34	15180	DR	11	2	VI	677777607760771	INH, STR	PAS
OO1	15758	BG	10	1	I	776177607763771	INH, STR	PAS
OO1	16054	CH	12	1	I	777777777763771	INH, RIF, EMB, STR	RMC, PAS
OO1	18048	CH	9	1	II	′000000000003771	INH, RIF, PZA, STR	RBT, RMC, PAS
BE	18460	MI	1	1	I	757777777413731	INH, RIF, EMB, STR	ETH, CYC, CIP, KAN, CAP, RBT, RMC, PAS
BE	17182	IN	1	1	I	777777777413731	INH	ETH, PAS
BE1	9560	IN	1	1	I	477777777413771	Susceptible	PAS
BE3	13310	IN	1	2	IV	777737777760771	INH, EMB, STR	PAS
BF53	16931	US	9	3	VII	′777777777760771	INH, STR	PAS
W	2550	US	18	1	II	′000000000003771	INH, RIF, EMB, PZA, STR	ETH, OFL, KAN, CYC, PAS
W	14003	RQ	18	1	II	′000000000003771	INH, RIF, EMB, STR	ETH, RBT, RMC, PAS
W269	15016	IN	14	1	II	′000000000003771	INH, RIF, EMB, PZA, STR	ETH, KAN, RBT, RMC, PAS
W283	14178	IN	14	1	II	′000000000003771	INH, RIF, EMB, PZA, STR	KAN, CAP, RBT, PAS
W563	18052	CH		1	II	′000000000003771	STR	PAS
HR102	19546	RP	10	1	I	677777477413771	INH, EMB, STR	PAS
HD15	18985	CH	11	1	II	′000000000003771	INH, RIF, EMB, PZA, STR	CYC, CIP, OFL, KAN, AMO, CAP, RBT, RMC, PAS
Clustered clinical isolates								
P	693	US	10	2	VI	′777777607760771	INH, RIF, EMB, PZA	ETH, PAS
P	758	US	10	2	VI	′777777607760771	INH, RIF, STR	ETH, KAN, CAP, CYC, PAS
P	768	US	10	2	VI	′777777607760771	INH, RIF, EMB, PZA, STR	ETH, PAS
P	1618	US	10	2	VI	′777777607760771	INH, RIF, EMB, STR	ETH, CIP, CAP, PAS
P	2557	US	10	2	VI	′777777607760771	INH, RIF, EMB, STR	CAP, PAS
P	3158	US	10	2	VI	′777777607760771	INH, RIF, EMB, PZA, STR	ETH, CIP, CAP, KAN, CYC, PAS
P	3814	US	10	2	VI	′777777607760771	INH, RIF	CIP, PAS[s]
P	5902	US	10	2	VI	′777777607760771	INH, RIF, PZA	PAS
P	8327	US	10	2	VI	′777777607760771	INH, RIF, EMB, PZA, STR	PAS
P	10454	US	10	2	VI	′777777607760771	NA	PAS
P	16442	RQ	10	2	VI	′777777607760771	INH, RIF, PZA, STR	RMC, PAS
P6	13249	US	10	2	VI	′777777607760771	INH, RIF, EMB, PZA, STR	PAS
P6	16796	US	10	2	VI	′777777607760771	INH, PZA	PAS
P23	16906	US	11	2	VI	′777777607760771	INH, RIF, EMB, PZA, STR	ETH, RMC, PAS
P	18137	US	10	2	VI	′777777607760771	INH, PZA, STR	PAS
P1	18900	US	11	2	VI	′777777607760771	INH, RIF, EMB, PZA	RBT, RMC, PAS
AB	1283	US	11	2	VI	676600000000371	INH, RIF, STR	PAS[s]
AB	6202	US	11	2	VI	676600000000371	INH, RIF, EMB, PZA	PAS
AB	1202	US	11	2	VI	676600000000371	INH, RIF	PAS

AB8	7958	US	11	2	VI	676600000000371	INH, RIF, EMB, STR	PAS
AU	2450	US	10	2	III	773777774020771	INH, RIF, EMB	PAS
AU	4718	US	10	2	III	773777774020771	RIF	CYC, PAS[s]
AU	4526	US	10	2	III	773777774020771	INH, RIF	PAS[s]
AU	1868	US	10	2	III	773777774020771	INH, RIF, EMB	PAS[s]
AU4	4619	US	11	2	III	773777774020771	Susceptible	PAS[s]
Reference susceptible clinical strains								
006	17994	US	0	ND	ND	777700000000000	Susceptible	PAS[s]
AF	9139	US	12	3	VIII	′777777777760771	Susceptible	PAS[s]
AI36	12556	RU	11	2	VI	′777760007760771	Susceptible	PAS[s]
BE	6921	US	1	1	I	ND	Susceptible	PAS[s]
CDC1551	5170	US	4	2	V	′700076757760771	Susceptible	PAS[s]
J	1694	US	12	3	VIII	′777777607560771	Susceptible	PAS[s]
W4	1147	US	18	1	II	′000000000003771	Susceptible	PAS[s]
Laboratory reference strains								
$H37Ra_1$	25177[i]	LAB	16	3	VIII	′777777477760771	Susceptible	PAS[s]
$H37Rv_2$	25618[i]	LAB	14	3	VIII	′777777477760771	Susceptible	PAS[s]
$H37Rv_2$	27294[i]	LAB	14	3	VIII	′777777477760771	Susceptible	PAS[s]
$H37Rv_2$	35821[i]	LAB	14	3	VIII	′777777477760771	Susceptible	PAS
$H37Rv_5$	35824[i]	LAB	13	3	VIII	′777777477760771	STR	PAS
$H37Rv_6$	35825[i]	LAB	14	3	VIII	′777777477760771	INH, STR	PAS
BCG-Branch	407[j]	LAB	1	1	I	ND	Susceptible	PAS[s]
BCG-Pasteur	35734[i]	LAB	1	1	I	ND	Susceptible	PAS[s]
M. bovis-NADL	410[j]	LAB	1	1	I	ND	Susceptible	PAS[s]
M .bovis-Rav	401[j]	LAB	1	1	I	ND	Susceptible	PAS[s]
M. africanum	5122[j]	LAB	ND	1	I	ND	Susceptible	PAS[s]
M . microti	19422[i]	LAB	ND	1	I	ND	Susceptible	PAS[s]

[a] FP, fingerprint name, based on IS6110 typing and PHRI nomenclature.
[b] TN, tracking number, a PHRI unique identifier for each isolate.
[c] ORI, country of origin (BG, Bangladesh; CH, China; DR, Dominican Republic; HA, Haiti; IN, India; KS, South Korea; MI, Malawi; RP, Philippines; RQ, Puerto Rico; RU, Russia; US, United States).
[d] No. of IS6110, number of IS6110 insertions in the isolate genome.
[e] PGG, principal genetic group (groups 1 to 3), based on polymorphisms in katG and gyrA.
[f] Cluster, genetic cluster (clusters I to VIII), based on 101 SNPs.
[g] Spoligo (octal), spoligotype, octal depiction.
[h] Resistance, drug susceptibility profile. INH, isoniazid; EMB, ethambutol; ETH, ethionamide; PZA, pyrazinamide; CYC, cycloserin; CIP, ciprofloxacin; OFL, ofloxacin; KAN, kanamycin; AMI, amikacin; CAP, capreomycin; RMC, rifamycin; RBT, rifabutin; ND, data not available.
[i] ATCC.
[j] Trudeau Mycobacterial Collection.

TABLE 2. Mutations associated with PAS resistance in reference strains and clustered and nonclustered clinical isolates ($n = 70$)[a]

Fingerprint (tracking no.)	PAS resistance[b]	No. of isolates	*thyA* mutation [amino acid/(SNP)]	*dfrA*	*folP2*
Reference strains					
Ra1; Rv2 (25618); Rv2 (27294)	S	3	WT[b]	WT	WT
Rv2 (35821); Rv5; Rv6	R	3	G91E (GGG→GAG)	WT	WT
M. microti, *M. africanum*	S	2	WT	WT	$^{-19}$A→G
BCG-Branch, BCG-Pasteur	S	2	WT	WT	$^{-19}$A→G
M. bovis-NADL, *M. bovis*-Ravenel	R	2	V263I (GTA-→ATA)	WT	$^{-19}$A→G
Clustered clinical isolates					
P strain 3814	S	1	WT	WT	WT
P (18137), P23 (16906) and P6 (13249)	R	3	T202A (ACC→GCC)	WT	WT
All other P strains from Table 1	R	10	T202A (ACC→GCC)/ ^{264}STOP→R (TGA→CGA)	WT	WT
P strain 3158	R	1	T202A (ACC→GCC)/ ^{264}STOP→R (TGA→CGA)	^{54}V→A/^{110}C→R	WT
P strain 693	R	1	T202A (ACC→GCC)/ ^{264}STOP→R (TGA→CGA)	^{66}S→C	WT
AB strain 1283	S	1	WT	WT	WT
AB strains 6202, 1202 and AB8 (7958)	R	3	T202A (ACC→GCC)	WT	WT
AU strains 4526 and 1868; AU4 strains 4718 and 4619	S	4	WT	WT	VNTR-Del
AU strain 2450	R	1	WT	WT	VNTR-Del
Nonclustered clinical isolates					
CDC1551 (5170), J (1694), 006 (17994), BE (6921), AF (9139), AI36 (12556), W4 (1147)	S	7	WT	WT	WT[c]
001 (15758)	R	1	V261G (GTC→GGC)	WT	WT
W283 (14178)	R	1	L183V (TTG→GTG)	WT	WT
BA19 (14303); BA19 (14550); BA27 (14204); BA34 (15180); CC3 (4469)	R	5	T202A (ACC→GCC)	WT	WT
A7 (6169); BE (17182); BE (18460); BE1 (9560); BE3 (13310)	R	5	WT	WT	$^{-19}$A→G
BF53 (16931); 001 (16054); 001 (18048); CI1 (4862); CI12 (18117); H (13528); H (14905); H (16213); HD15 (18985); HR102 (19546); W (14003); W563 (18052); W (2550); W269 (15016)	R	14	WT	WT	WT

[a] The DNA of all isolates includes wild-type (WT) *thyX*, *folP*, *folC*, *nhoA*, *aac(1)*, and *aac(2)* genes and flanking region.
[b] PAS-resistant (R) and -susceptible (S) phenotypes.
[c] Strains 006 (17994) and BE (6921), $^{-19}$A→G.

and corresponding upstream regions (~100 nt upstream) were sequenced for 12 reference strains (Table 2), 3 groups of clustered strains (Table 2), and 55 spontaneous mutants (Table 3). In total, 118 samples were sequenced (Table 1). Drug susceptibility profiles were also determined for each isolate. To generate spontaneous mutants, all parental strains were drug susceptible except for a mono-rifampin-resistant AU4718 strain (2).

Mutations in the *dfrA*, *folP1*/*folP2*, and *thyX* genes are not associated with PAS resistance. Three mutations in the *dfrA* gene (^{66}S→C, ^{54}V→A, and ^{110}C→R) were identified in two clinical isolates that in addition already bore a mutation in the *thyA* gene (Table 2). Specifically, strain P-3158 encoded SNP ^{66}S→C, while P-693 included two mutations in the *dfrA* gene (^{54}V→A and ^{110}C→R). No PAS^r isolate with a polymorphism only within the *dfrA* gene was found; consequently, it is not known whether the three *dfrA* mutations alone contribute to a PAS^r phenotype. No mutations were found within the *thyX* gene or flanking regions in either the clinical isolates or the spontaneous mutants. This gene is also highly conserved (100%) among other *M. tuberculosis* complex strains (GenBank database; data not shown). Likewise, the *folP1* gene and flanking sequences were conserved throughout, while some polymorphisms were noted in the *folP2* gene and its upstream region. FolP2 has been listed as a nonessential enzyme by transposon mutagenesis (28). A single-nucleotide substitution was found upstream from the starting codon of *folP2* ($^{-19}$A→G) in both PAS^s and PAS^r isolates. This single-nucleotide polymorphism (SNP) is also present in PAS$^{r/s}$ *M. bovis* and *M. bovis* BCG. All isolates characterized by this SNP grouped in genetic cluster I (9) and were correlated with a phylogenetic lineage, rather than PAS resistance. The N terminus of the *folP2* gene comprises three and a half imperfect 27-nt-long tandem repeats, except for PAS$^{r/s}$ AU strains. All AU strains have lost most of the second repeat while retaining the coding region in frame. The observation that both PAS$^{r/s}$ AU isolates carry this alteration indicates that this mutation is not associated with PAS^r, but rather, is a molecular characteristic of AU and related strains. Thus, no mutations within the genes encoding enzymes in the folate and thymine biosynthetic

TABLE 3. Mutations in the *thyA* gene associated with PAS resistance in spontaneous mutants ($n = 55$)[a]

Fingerprint (tracking no.)	PAS resistance[d]	No. of isolates	*thyA* mutation [codon (amino acid)]	*folP2* mutation
(A)[b]	R	24	WT	WT
(B)[c]	R	10	WT	$^{-19}$A→G
BE_149	R	1	TGG→TAG (W83STOP)	$^{-19}$A→G
AF_62/AF_52	R	2	CAG→TAG (Q111STOP)	WT
BE_147	R	1	TTG→TAG (L118STOP)	$^{-19}$A→G
BE_43	R	1	TAC→TAA (Y153STOP)	$^{-19}$A→G
BE_148	R	1	TAC→TAA (Y164STOP)	$^{-19}$A→G
OO6_160	R	1	TAC→TAG (Y251STOP)	WT
W4_22	R	1	INS 2 ntds; Frameshift 11	WT
OO6_15	R	1	DEL 5 ntds; Frameshift 72	$^{-19}$A→G
W4_3	R	1	DEL 2 ntds; Frameshift 217	WT
OO6_79	R	1	GGT→CGT (G15R)	WT
OO6_18	R	1	GGG→AGG (G91R)	$^{-19}$A→G
OO6_10	R	1	CGC→CTC (R127L)	$^{-19}$A→G
AI_64	R	1	CTG→CCG (L143P)	WT
J_152	R	1	TGT→CGT (C146R)	WT
BE_144	R	1	CTG→CCG (L172P)	$^{-19}$A→G
AI_163	R	1	GCG→CCG (A182P)	WT
OO6_17	R	1	CAG→CGG (Q191R)	$^{-19}$A→G
CDC-10	R	1	ACC→GCC (T202A)	WT
AU_121	R	1	GCT→CCT (A259P)	WT
CDC_78	R	1	GTA→GGA (V263G)	WT

[a] Isolates are ordered by mutation codon number from the N to C terminus. All are PAS^r spontaneous mutants with wild-type (WT) *thyX*, *dfrA*, *folP1*, *folC*, *nhoA*, *aac(1)*, and *aac(2)* genes and flanking regions.

[b] PAS^r spontaneous mutants with wild-type *thyA* gene.

[c] PAS^r spontaneous mutants as in (B) with an additional SNP upstream of *folP2* not associated with PAS resistance.

[d] R, resistant.

pathway, other than *thyA*, were correlated with a PAS^r phenotype. Additionally, no SNPs were identified in *folC* (Rv2447c) and three *N*-acetyltransferase genes, including *nhoA* (Rv3566c), *aac(1)* (Rv0262), and *aac(2)* (Rv1347c).

Thirty-seven percent of PAS^r strains have a mutation within the thymidylate synthase A (*thyA*) gene. Sequence analysis of the clinical isolates and spontaneous mutants revealed 24 different mutations in the *thyA* gene, including 4 and 20 distinct polymorphisms in clinical isolates and spontaneous mutants, respectively (Tables 2 and 3). It is noteworthy that most polymorphisms found in the clinical isolates and the spontaneous mutants were distinct. Only the most common mutation identified in clinical isolates (^{202}ACC→GCC; ^{202}T→A) was also identified in a single spontaneous mutant. This SNP was characteristic of all PAS^r clinical isolates belonging to two unrelated strain clusters (genotypes P and AB), as well as an additional four strains accounting for six different genotypes altogether (Table 2), but was not found in corresponding related PAS^s isolates. The mutation ^{91}GGG→GAG (^{91}G→E) was identified in all three laboratory PAS^r H37Rv isolates, but not in the PAS^s H37Rv/a. The three PAS^r H37Rv isolates were generated by Steenken and Wolinsky in the 1950s (30). Interestingly, a different SNP was identified at the same position (^{91}GGG→AGG; ^{91}G→R) in a single spontaneous mutant. Other SNPs, deletions, or insertions leading to either stop codons or frameshifts were noted among the spontaneous mutants (Table 3). Other polymorphisms in the *thyA* gene were distributed throughout the gene. Although no "hot spot" drug resistance-determining region within the *thyA* gene was identified, protein structural predictions indicate that all the mutations recorded reside within essential functional or structural sites, as discussed below (Table 4). An unexpectedly high number of PAS^r isolates were found to have wild-type genotypes for the enzymes of the folate and thymidine biosynthetic pathways among clinical isolates and the spontaneous mutants.

PAS^r *M. tuberculosis* P strains have dual mutations in *thyA*. Fifteen isolates known to be PAS^r and one PAS^s isolate belonging to a single cluster known as the P strain family were analyzed. These isolates belong to a larger cluster of over 120 isolates associated with MDR outbreaks in New York City and neighboring states (21). One isolate sharing the same molecular genotype and resistance phenotype (rifampin and isoniazid resistance) as the other P strains was found to be PAS^s and hence was used as a control strain. The 15 PAS^r P strains had a characteristic mutation in codon 202 (^{202}T→A) of *thyA*, and 12 of them had a second mutation in the *thyA* gene consisting of a single-nucleotide substitution at the termination codon (^{264}TGA→CGA; ^{264}stop→R) (Table 2). A hairpin structure 3 nt downstream from the stop codon could function as a terminator of the mRNA, allowing *dfrA* transcript initiation. It is unlikely that *thyA-dfrA* forms an operon. A putative ribosome binding site is present 15 nt upstream from the *dfrA* gene. Alternatively, an unlikely run-through transcript would result in an extended *thyA* mRNA overlapping out of frame by 251 nt with the downstream coding region of the *dfrA* gene. These data suggest that the P strain acquired the ^{202}ACC→GCC mutation prior to the mutation in the termination codon. Moreover the identification of mutation 202 alone in two closely related P variants (P6 and P23) indicates that these isolates diverged after the acquisition of mutation 202 but prior to the acquisition of the SNP on the termination codon. Two of the double-ThyA-mutant P strains developed secondary mutations on the flanking *dfrA* gene (^{66}S→C and a double mutation, ^{54}V→A and ^{110}C→R, on a second strain), as described above.

Predicting the structural implications of the *thyA* mutations identified. To understand the impacts of the identified mutations on protein function, a 3D homodimer structure of *M. tuberculosis* thymidylate synthase was modeled based on the X-ray structure of the *E. coli* thymidylate synthase as a homologous template. *M. tuberculosis* and *E. coli* ThyA protein sequences share strong identity (67%) and similarity (83%). The model showed an equivalent resolution of 1.7 Å according to hydrogen bond energy criteria, with no residue found in the disallowed regions of the Ramachandran plot. Analysis of the mutations positioned within the structure model revealed three groups of mutants (Table 4 and Fig. 2).

The first group (Fig. 2) consists of mutations that modify the length of the protein. Six stop mutations (^{83}W→stop, ^{111}Q→stop, ^{118}L→stop, ^{153}Y→stop, ^{164}Y→stop, and ^{251}Y→stop) and three insertion/deletion alterations, including 5- and 2-nt deletions and a 2-nt insertion in codons 11, 72, and 217, respectively, introduce early frameshift. Such modifications are expected to render the enzyme nonfunctional due to the loss of its ternary structure, which harbors many residues of active sites or of cofactor binding sites located within the C-terminal part of the enzyme. A 10th mutation potentially extending the size of the protein by 76 amino acids through the obliteration of the stop codon was also identified in the P clinical cluster. Existing structural data on other bacterial and eukaryotic ThyA enzymes have shown that the C-terminal amino acid has a functional role in catalysis (Fig. 2).

The second group of mutants contains mutations of amino

TABLE 4. Features of PAS^r *thyA* mutants

Mutant	$\Delta\Delta G$[a]	MIC[b]	Cons[c]	Structural features
Truncated protein mutants				
83W→Stop		>128		Truncated polypeptide
111Q→Stop		>128		Truncated polypeptide
118L→Stop		>128		Truncated polypeptide
153Y→Stop		>128		Truncated polypeptide
164Y→Stop		>128		Truncated polypeptide
251Y→Stop		>128		Truncated polypeptide
264Stop→R		>128		Truncated polypeptide
Mutations affecting catalytic site				
127R→L	+0.18	>128	99.2 (0)	In interaction with substrate dUMP
143L→P	+2.45	>128	98.9 (0)	In interaction with THF cofactor
146C→R	+1.56	>128	100 (0)	Catalytic residue
172L→P	+1.28	>128	99.2 (0)	In interaction with THF cofactor
182A→P	+3.94	>128	77.6 (0)	Completely buried into the hydrophobic core of the enzyme
259A→P	+1.56	<64	55.1 (0)	Close to the binding site of cofactor folate derivative
261V→G	+0.52	>128	43.0 (0)	In interaction with THF cofactor
263V→I	+0.45	ND	80.5 (10)	Close to binding site of THF cofactor
Structurally destabilized mutants				
15G→R	+1.20	>8 <32	99.5 (0)	Makes 1-residue-long link between two secondary structures
91G→E	+1.68	ND	99.2 (0)	Buried and in positive backbone j torsion angle
91G→R	+1.89	ND	99.2 (0)	Buried and in positive backbone j torsion angle
183L→V	+2.13	<64	80.7 (0)	Completely buried into the hydrophobic core of the enzyme
191Q→R	+1.39	<64	20.6 (0)	Buried residue in C-terminal region of an α-helix
202T→A	+3.24	<128	70.2 (1)	In dimeric interface opposite to the equivalent residue

[a] $\Delta\Delta G$ (in kcal/mol) is the predicted change in folding free energy upon single-site mutation computed on an *M. tuberculosis* homodimer 3D model with the PoPMuSiC program (13). The computed values were averaged on both chains.
[b] In μg/ml. ND, not determined.
[c] Cons is the conservation percentage of a given residue as determined from the multiple-amino-acid alignment of 279 different ThyA sequences. Mutant residues are in parentheses.

acids involved in the active catalytic site or within the cofactor or substrate binding site (Fig. 2). For example, mutation ^{127}R→L affects the residue involved in dUMP substrate binding, while ^{172}L→P, ^{143}L→P, ^{261}V→G, and ^{263}V→I interact with the folate derivative. ^{146}C→R forms part of the catalytic site.

The third group encompasses mutations that could destabilize the ternary structure of the ThyA protein (Fig. 2), rendering the enzyme dysfunctional or less active (26). Mutants with ^{15}G→R, ^{91}G→E, and ^{91}G→R mutations change glycine residues otherwise conserved among all known thymidylate synthase structures to satisfy conformational restraints. Residues ^{82}Ala and ^{183}Leu are completely embedded in the hydrophobic clusters of the protein core. ^{202}Thr is an amino acid located at the monomer-monomer interface facing the ^{202}Thr of its counterpart. Therefore, all mutants were predicted to encode destabilizing mutations, according to the positive changes of free folding energy computed by the PoPMuSiC program (Table 4).

Elevated MICs in PAS^r spontaneous mutants and clinical isolates. The MICs of selected clinical isolates and spontaneous mutants were determined by the dilution assay and Bactec/Alert culture (Table 4). In a departure from the conventional application of Bactec/Alert for diagnostic purposes, the growth of PAS^r samples was followed over a period of 2 weeks in the presence of increasing concentrations of PAS. Samples including mutations within the *thyA* gene proved to be highly resistant to PAS. This observation was further confirmed by plating the samples at various concentrations of PAS (up to 128 μg/ml).

In addition, the growth curves of representative PAS^r samples were followed in triplicate over a period of 32 days (Fig. 3). The growth curve profiles of strains with a mutated ThyA protein, which were found to be equally resistant to increasing concentrations of PAS up to the 128 μg/ml tested, were noteworthy, displaying overlap with the corresponding untreated strains. In contrast, the growth of PAS^r isolates encoding wild-type proteins of the folate pathway was found to be dose dependent. For these isolates, growth was proportionally inhibited as the dose of PAS was increased, clearly indicating the presence of a different mechanism of PAS resistance.

DISCUSSION

Recently, the *thyA* gene of the folate pathway was shown to be associated with PAS resistance in *M. tuberculosis* (26). In the present study, we analyzed the *thyA* sequences in 118 strains, including references strains, clinically diverse and clustered PAS^r strains, and PAS^r spontaneous mutants, and found that only 37% of the samples included a *thyA* mutation implicated in PAS resistance. The limited association between the PAS^r phenotype and mutations in the *thyA* gene led us to examine the nucleotide sequences of five other enzymes in the folate pathway and thymine biosynthesis, as well as three *N*-acetyltransferase genes. To our surprise no mutations were identified in these eight genes.

Twenty-four distinct mutations were identified in the *thyA* gene, including 4 SNPs found uniquely in clinical isolates and 20 observed in the spontaneous mutants. A single polymor-

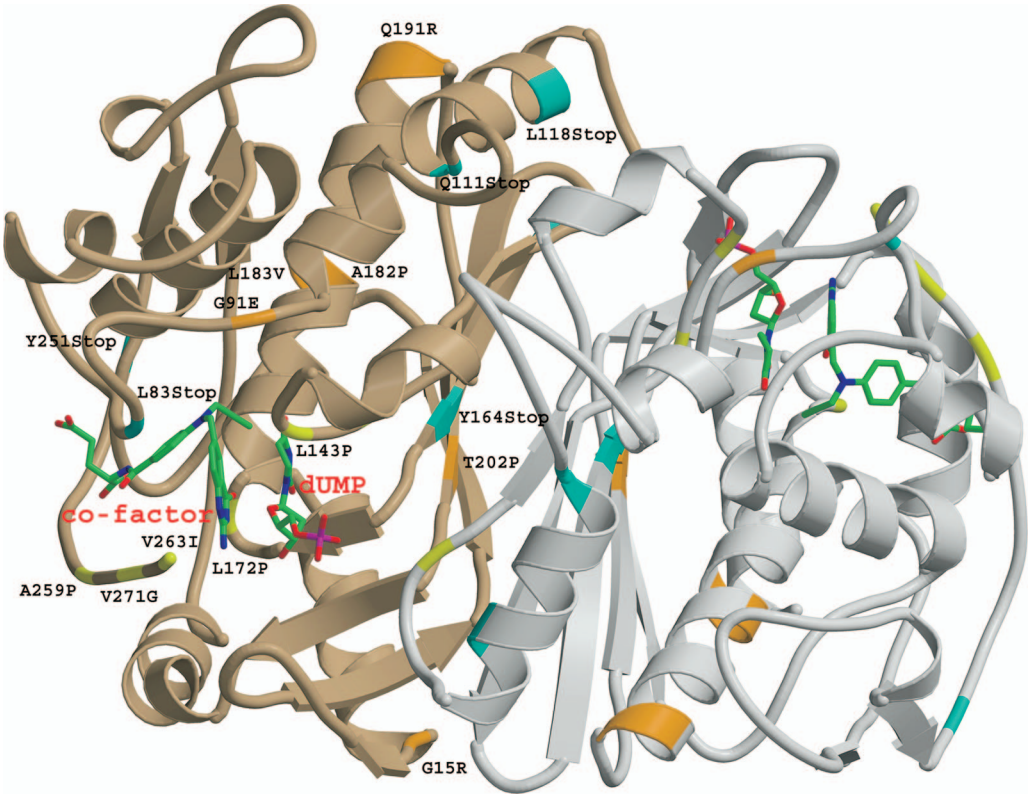

FIG. 2. Ribbon view of a homodimer model of the *M. tuberculosis* thymidylate synthase enzyme. The mutated positions are labeled and depicted in one monomer and colored coded in the other monomer. Blue, stop codon mutations; orange, mutations affecting protein stability; yellow, mutations of residues involved in substrate or cofactor binding. The dUMP substrate and folate cofactor are also depicted and labeled in red.

phism (^{202}ACC→GCC), previously reported, was seen in clinical isolates and one spontaneous mutant (26). The divergence in mutation type observed in clinical isolates and spontaneous mutants could result from experimental bias due to PAS^r selection at elevated concentrations of PAS or to the limited number of PAS^r isolates investigated. Alternatively, ThyA may not be an essential enzyme in vitro while assuming a more significant function in vivo. This could be due to a higher demand in vivo for thymine, lower availability of extracellular thymine, or even a functional difference in the complementary ThyX, which may require complementation for an active ThyA. The observation that nine of the spontaneous mutants encoded truncated ThyA proteins supports this notion; however, further work is needed to confirm this possibility. Other mutations in ThyA among the spontaneous mutants were found to be equally destabilizing. They include alterations affecting the substrate or cofactor binding site or the catalytic site or resulting in major structural changes as determined by analysis of predicted 3D-mutated ThyA.

The most prevalent mutation, ^{202}ACC→GCC, was found in spontaneous mutants and molecularly/epidemiologically unrelated clinical isolates ($n = 4$), as well as in strain clusters belonging to P and AB genotypes. Sequence analysis of the P strain cluster isolates revealed that all resistant samples had the characteristic ^{202}ACC→GCC mutation and that 12 of them additionally included a stop codon, suggesting sequential acquisition. The deletion of the stop codon alone was not shown to be associated with PAS^r, as no isolates with the obliterated ^{264}stop codon alone were identified. Structural predictions of the ThyA protein and literature review suggest that the carboxyl-terminal amino acid folds back into the catalytic groove of the enzyme and therefore may be functionally relevant.

Overall, protein structure modeling predicts that all 24 different mutations identified in the *thyA* gene map to essential amino acids affecting either the structure, the functional site (substrate, cofactor binding site, or catalytic site), or the dimer interface of the ThyA homodimer. Six mutations were found in key positions of spatial structure, radically altering the conformation of the enzyme. Seven of the mutations involved essential amino acids in close proximity to the catalytic site, including a PAS^r spontaneous mutant with a single point mutation in amino acids of the catalytic site (^{261}V→G and ^{263}V→I) and mutant ^{127}R→L, encoding an amino acid substitution at the substrate dUMP binding site.

The observation that most mutants reported here affect highly conserved positions otherwise rarely found in the protein family of thymidylate synthase is noteworthy. Our results indicate that the observed mutations affect residues under strong functional selection that are uncommon in nature (Table 4). This detrimental alteration to ThyA is permissible in *M. tuberculosis* due to the presence of the complementary functional homologue ThyX. ThyX per se does not seem to be susceptible to PAS. This is further exemplified in the work of Rengarajan and colleagues, who have shown that the resistant phenotype of transposon-generated PAS^r mutants could be

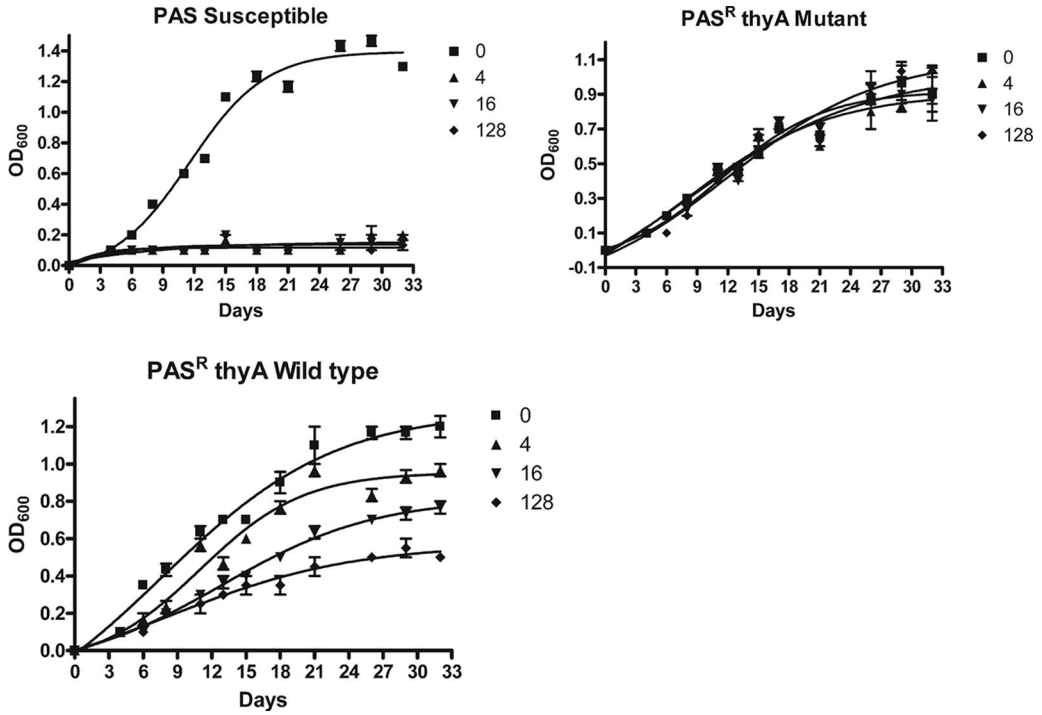

FIG. 3. Representative growth curves of PAS^s and PAS^r isolates in the presence of various concentrations of PAS (in μg/ml). PAS^r isolates with a mutated *thyA* gene (truncated or with an altered catalytic site) were equally resistant to increasing concentrations of PAS, while PAS^r isolates with a wild-type genotype were dose dependent. For this isolate, growth was inhibited at increasing concentrations of PAS. The error bars indicate standard deviations of three independent experiments. OD_{600}, optical density at 600 nm.

reversed through complementation/overexpression of the wild-type *thyA* gene (26).

Mutations in the *thyA* gene were associated with elevated levels of PAS resistance, as determined by dilution assays, Bactec/Alert susceptibility testing, and growth curve experiments. Interestingly, spontaneous mutants encoding a ThyA modification responded equally to increasing concentrations of PAS, while PAS^r mutants encoding wild-type ThyA proved to be dose dependent. This observation indicates that the yet unidentified alternative mechanism(s) or target(s) associated with PAS^r is concentration dependent.

The observation that PAS is active only in the presence of a functional ThyA enzyme suggests that, like other antimycobacterials (isoniazid, ethionamide, and pyrizinamide), PAS is a prodrug whose activation somehow requires a viable ThyA, as was also previously proposed (26).

ACKNOWLEDGMENTS

V.M. is the recipient of a doctoral scholarship from the FNRS (Belgian Fund for Scientific Research). R.W. is a Research Associate at the FNRS. A.S. is supported by the Novartis Institute for Tropical Diseases, NITD. This work was supported in part by Les Amis de L'Institut Pasteur de Bruxelles. We thank bioMérieux Belgium for sponsoring the MIC determinations by Bactec/Alert and for technical support.

We are grateful to J. Rengarajan and E. Rubin, Harvard School of Public Health, Boston, MA, for insightful suggestions during the course of the work.

REFERENCES

1. **Altschul, S. F., W. Gish, W. Miller, E. W. Myers, and D. J. Lipman.** 1990. Basic local alignment search tool. J. Mol. Biol. **215:**403–410.
2. **Bifani, P., B. Mathema, N. E. Kurepina, E. Shashkina, J. Quatannens, A. S. Blanchis, S. Moghazeh, J. Driscoll, B. Gicquel, R. Frothingham, and B. N. Kreiswirth.** 2008. The evolution of drug-resistance in *Mycobacterium tuberculosis*: from a mono-rifampin resistant cluster into increasingly multidrug resistant variants in an HIV sero-positive population. J. Infect. Dis. **198:**90–94.
3. **Bifani, P., S. Moghazeh, B. Shopsin, J. Driscoll, A. Ravikovitch, and B. N. Kreiswirth.** 2000. Molecular characterization of *Mycobacterium tuberculosis* H37Rv/Ra variants: distinguishing the mycobacterial laboratory strain. J. Clin. Microbiol. **38:**3200–3204.
4. **CDC.** 1992. Update: availability of streptomycin and para-aminosalicylic acid—Unites States. MMWR Morb. Mortal. Wkly. Rep. **41:**482.
5. **De Logu, A., V. Onnis, B. Saddi, C. Congiu, M. L. Schivo, and M. T. Cocco.** 2002. Activity of a new class of isonicotinoylhydrazones used alone and in combination with isoniazid, rifampicin, ethambutol, para-aminosalicylic acid and clofazimine against *Mycobacterium tuberculosis*. J. Antimicrob. Chemother. **49:**275–282.
6. **Fisher, B. M., G. Roberts, and H. C. Hinshaw.** 1951. The subcutaneous administration of the sodium salt of para-aminosalicylic acid in the treatment of tuberculosis. Am. Rev. Tuberc. **64:**557–563.
7. **Gilis, D., and M. Rooman.** 2000. PoPMuSiC, an algorithm for predicting protein mutant stability changes: application to prion proteins. Protein Eng. **13:**849–856.
8. **Graziani, S., J. Bernauer, S. Skouloubris, M. Graille, C. Z. Zhou, C. Marchand, P. Decottignies, H. van Tilbeurgh, H. Myllykallio, and U. Liebl.** 2006. Catalytic mechanism and structure of viral flavin-dependent thymidylate synthase ThyX. J. Biol. Chem. **281:**24048–24057.
9. **Gutacker, M. M., B. Mathema, H. Soini, E. Shashkina, B. N. Kreiswirth, E. A. Graviss, and J. M. Musser.** 2006. Single-nucleotide polymorphism-based population genetic analysis of *Mycobacterium tuberculosis* strains from 4 geographic sites. J. Infect. Dis. **193:**121–128.
10. **Gutacker, M. M., J. C. Smoot, C. A. Migliaccio, S. M. Ricklefs, S. Hua, D. V. Cousins, E. A. Graviss, E. Shashkina, B. N. Kreiswirth, and J. M. Musser.** 2002. Genome-wide analysis of synonymous single nucleotide polymorphisms in *Mycobacterium tuberculosis* complex organisms: resolution of genetic relationships among closely related microbial strains. Genetics **162:** 1533–1543.
11. **Hubbard, S. J., and J. M. Thornton.** 1993. NACCESS Computer Program. University College, London, United Kingdom.
12. **Kunz, B. A., and S. E. Kohalmi.** 1991. Modulation of mutagenesis by deoxyribonucleotide levels. Annu. Rev. Genet. **25:**339–359.

13. **Kwasigroch, J. M., D. Gilis, Y. Dehouck, and M. Rooman.** 2002. PoPMuSiC, rationally designing point mutations in protein structures. Bioinformatics **18:**1701–1702.
14. **Laskowski, R. A., J. A. Rullmannn, M. W. MacArthur, R. Kaptein, and J. M. Thornton.** 1996. AQUA and PROCHECK-NMR: programs for checking the quality of protein structures solved by NMR. J. Biomol. NMR **8:**477–486.
15. **Lehmann, J.** 1946. Para-aminosalicylic acid in the treatment of tuberculosis. Lancet **247:**15–16.
16. **Lehmann, J.** 1949. The treatment of tuberculosis in Sweden with para-aminosalicylic acid; a review. Dis. Chest **16:**684–703.
17. **Luria, S. E., and M. Delbruck.** 1943. Mutations of bacteria from virus sensitivity to virus resistance. Genetics **28:**491–511.
18. **Mathema, B., N. E. Kurepina, P. J. Bifani, and B. N. Kreiswirth.** 2006. Molecular epidemiology of tuberculosis: current insights. Clin. Microbiol. Rev. **19:**658–685.
19. **Medical Research Council.** 1949. Treatment of pulmonary tuberculosis with para-aminosalicylic acid and streptomycin. Br. Med. J. **2:**1521.
20. **Morlock, G. P., J. T. Crawford, W. R. Butler, S. E. Brim, D. Sikes, G. H. Mazurek, C. L. Woodley, and R. C. Cooksey.** 2000. Phenotypic characterization of *pncA* mutants of *Mycobacterium tuberculosis*. Antimicrob. Agents Chemother. **44:**2291–2295.
21. **Munsiff, S. S., T. Bassoff, B. Nivin, J. Li, A. Sharma, P. Bifani, B. Mathema, J. Driscoll, and B. N. Kreiswirth.** 2002. Molecular epidemiology of multidrug-resistant tuberculosis, New York City, 1995–1997. Emerg. Infect. Dis. **8:**1230–1238.
22. **Murray, J. F.** 2004. A century of tuberculosis. Am. J. Respir. Crit. Care Med. **169:**1181–1186.
23. **Newby, Z., T. T. Lee, R. J. Morse, Y. Liu, L. Liu, P. Venkatraman, D. V. Santi, J. S. Finer-Moore, and R. M. Stroud.** 2006. The role of protein dynamics in thymidylate synthase catalysis: variants of conserved 2′-deoxyuridine 5′-monophosphate (dUMP)-binding Tyr-261. Biochemistry **45:**7415–7428.
24. **Nopponpunth, V., W. Sirawaraporn, P. J. Greene, and D. V. Santi.** 1999. Cloning and expression of *Mycobacterium tuberculosis* and *Mycobacterium leprae* dihydropteroate synthase in *Escherichia coli*. J. Bacteriol. **181:**6814–6821.
25. **Pugh, D. L., G. S. Edwords, R. G. McLaren, and E. R. Jones.** 1952. Toxic psychiatric manifestations in the treatment of tuberculosis with sodium para-aminosalicylate. Tubercle **33:**369–376.
26. **Rengarajan, J., C. M. Sassetti, V. Naroditskaya, A. Sloutsky, B. R. Bloom, and E. J. Rubin.** 2004. The folate pathway is a target for resistance to the drug para-aminosalicylic acid (PAS) in mycobacteria. Mol. Microbiol. **53:**275–282.
27. **Sali, A., and T. L. Blundell.** 1993. Comparative protein modelling by satisfaction of spatial restraints. J. Mol. Biol. **234:**779–815.
28. **Sassetti, C. M., D. H. Boyd, and E. J. Rubin.** 2003. Genes required for mycobacterial growth defined by high density mutagenesis. Mol. Microbiol. **48:**77–84.
29. **Steenken, W., Jr., and E. Wolinsky.** 1956. Cycloserine: antituberculous activity *in vitro* and in the experimental animal. Am. Rev. Tuberc. **73:**539–546.
30. **Steenken, W., Jr., and E. Wolinsky.** 1950. Effects of antimicrobial agents on the tubercle bacillus and on experimental tuberculosis. Am. J. Med. **9:**633–653.
31. **Therapeutic Trials Committee of the Swedish National Association against Tuberculosis.** 1950. Para-aminosalicylic acid treatment in pulmonary tuberculosis. Am. Rev. Tuberc. **61:**597–612.
32. **Thompson, J. D., T. J. Gibson, F. Plewniak, F. Jeanmougin, and D. G. Higgins.** 1997. The CLUSTAL_X windows interface: flexible strategies for multiple sequence alignment aided by quality analysis tools. Nucleic Acids Res. **25:**4876–4882.
33. **Wallace, A. C., R. A. Laskowski, and J. M. Thornton.** 1995. LIGPLOT: a program to generate schematic diagrams of protein-ligand interactions. Protein Eng. **8:**127–134.
34. **WHO.** 2000. Guidelines for establishing DOTS-Plus pilot projects for the management of multidrug-resistant tuberculosis (MDR-TB). WHO/CDS/TB/2000.279. WHO, Geneva, Switzerland.